The effect of operating conditions on post-injection fuel discharge in an optical engine

J. E. Turner[a], V. Stretsyuk[a], C. Crua[a,1], M. R. Gold[b], R. J. Pearson[b]
[a] Centre for Automotive Engineering, University of Brighton, Brighton BN2 4GJ, UK
[b] BP Global Fuels Technology, Pangbourne, RG8 7QR, UK

Abstract

After the end of injection, the needle closes and residual fuel present inside the injector sac and orifices is discharged due to the high fluid inertia. This so-called post-injection fuel discharge can present several problems. The excess fuel can undergo incomplete combustion due to its large, slow moving and often surface-bound nature. Not only does this have a negative effect on emissions and performance, but it has been speculated that the by-products of incomplete combustion are implicated in the growth of carbonaceous deposits on the tips of fuel injectors. Accumulation of these deposits is known to lead to premature fuel injector failure that can lead to reductions in power output and engine lifetime. Seeing as modern multiple-injection strategies give rise to an increased number of transient injection phases, post-injection discharges are an increasingly common occurrence during normal operating conditions. In order to develop a phenomenological model for the fluid dynamics after the end of injection, there is a need to characterise the causes of this discharge and how they might be influenced by engine operating conditions. In this study we present ongoing analysis into results from the first visualisation of post injection fuel discharge at the microscopic level under engine-like operating conditions. We observed the process of fuel discharge for multi-hole injectors, using a high-speed camera fitted with a long-distance microscope and a high-speed laser illumination source. We related the effect of a variety of operating conditions on the severity of this process, including injection pressure and in-cylinder pressure along with a characterisation of the dynamics of the various modes by which these undesired liquid structures are produced. We present the different modes by which this process occurs and we conclude that the extent of post-injection discharge depends on both the in-cylinder and injection pressures.

Keywords: Spray, atomization, post-injection discharge, injection, optical diagnostics

Introduction

In order to meet increasingly stringent emission standards, the automotive industry has been modifying various parameters of the Fuel Injection Equipment (FIE). This has meant common rail pressures and the numbers of holes in the injector tip are increasing with subsequent designs, often with systems capable of common rail pressures of 300 MPa [1]. Pressure regulation systems in the common rail require that some of the fuel undergoes expansion, which causes some of the fluid's energy to be dissipated as heat leading to even higher fuel temperatures [2]. These harsh conditions are thought to accelerate the formation and growth of deposits which is known to manifest in a variety of ways including increased emissions, smoke, injector sticking and engine failure [3,4].

The increased use of piezo-actuated injectors is another way of optimising injection systems. With piezo-actuated injectors, post-injections are isolated much better due to the faster dynamic response when compared to older traditional solenoid systems. This is a result of the ability of a piezo stack to generate forces of 800N as opposed less than 100N as is often the case with older systems [5]. These older systems are known to show decreased liquid penetration and therefore less efficient fuel-air mixing processes [6], but despite the significant capacity to reduce particulate emissions whilst retaining engine performance, these problems still remain.

Another key strategy in optimisation is the moving towards split injection cycles as a means of controlling the rate of injection and the fuel-air mixing process. This means that some transient phases of the injection process occur much more frequently with these new systems. It is already known that these early and late phases of the injection produce large, slow, deformed and often surface-bound liquid structures. With a split injection strategy, these large liquid structures will be formed in a combusting environment and are therefore expected have a notable effect on not only particulate emissions, but these structures are also likely to be involved in the formation of carbonaceous deposits on and around the injector orifices. One notable transient effect that has gained attention more recently is so-called post-injection-fuel discharge.

If there is a link between observable fluid on and around the injector orifices, then an investigation into such behaviour would help solve the long standing issue of deposit formation in engines. Deposits within the nozzle holes of injectors can affect the engine performance in a variety of ways. Acoustic emissions can increase [7] as well as pollutant emissions [8, 9]. The deposits can reduce the hydraulic diameter of the nozzle hole and, therefore,

[1] Corresponding author: c.crua@brighton.ac.uk

fuel flow from the nozzle. This can result in a reduction on the quantity of injected fuel and reduced quality of injection [9-11], which causes a reduction in engine power [2]. The deposits can also lead to cavitation, which can then lead to further coking of the nozzle [12]. To further compound these issues, the strict tolerances of critical parts of the FIE and the changes in fuel composition have reduced the fuels ability to dissolve these deposits. Caprotti et al. [9] hypothesised that fluid expansion in the nozzles at the end of injection could be involved in the formation of deposits. In order to investigate these assumptions, experimental non-intrusive methods are required to observe the fluid dynamics on and around the injector nozzles.

In this research we performed the first visualisation of post-injection fuel discharge at the microscopic level. By doing this we were able to gain insight into fluid dynamics that are believed to influence fuel-air mixing and emissions as well as being implicated in the formation of deposits on and around the nozzle holes. The main focus of this investigation is to ask "are external fluid dynamics inside and around injector holes implicated in the formation and growth of internal deposits?"

Experimental Methods

A single cylinder reciprocating rapid compression machine (RCM) was used in the present research. The RCM was a single-cylinder, two-stroke engine of 135x150 mm with a displacement of 2.2 litres. The fuel injection equipment consisted of a number of classical common rail components. The high pressure fuel pump was an electrically driven pump connected to a common rail system capable of delivering a rail pressure of up to 200 MPa.

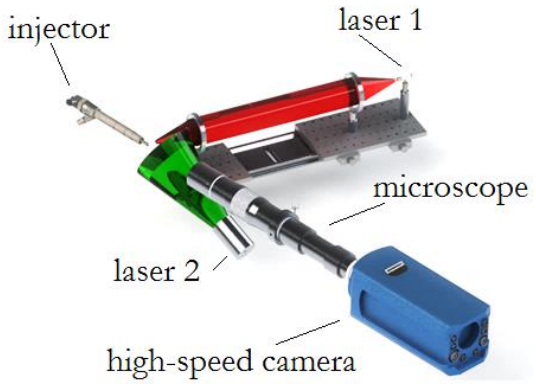

Figure 1: Experimental setup used to study fuel dynamics at the end of injection around injector tip. Double illumination configuration was used.

Operating conditions were chosen to represent idle to medium engine load. In-cylinder pressures (ICP) were 40 to 80 bar in steps of 10 and injection pressures were 400, 700 and 1000 bar. Estimated in-cylinder temperature was in the range of 700-760 K. Fuel used was conventional diesel fuel (B0). The fuel was injected for 500 µs (TTL trigger duration) at 3° before top dead centre (bTDC) and the high speed clips were captured at different times after the start of injection (0.3-1.5 ms). Ambient conditions are defined as atmospheric pressure and temperature where the only variable is injection pressure. The camera used was a phantom v12.1 12 bit high-speed CCD camera recording at 160x152 pixels resolution for a total of 85 frames which allowed a maximum frame rate of 100kfs. Scale factor was 3.48 µm/pixel to give a field of view of 529 µm x 557µm. Illumination was first achieved using a CAVILUX Cavitar 690 nm solid state diode laser. For later experiments the dual-illumination setup was used with an external trigger being provided by a pulse generator. Visualisation of a single hole at higher resolution under atmospheric operating conditions was performed by using a Delphi DFI 1.5 8 hole injector.

Data-processing

High speed video clips were acquired by using 12 bit CCD camera and processed using MATLAB. The post processing algorithm is based on the analysis of mean and standard deviation of recorded intensity for a region of interest in each frame. The intensity is then normalised to the first 'reference' frame. The result is a plot of mean and standard deviation of intensity, as a function of frame number, time after the start of injection and crank angle. The post processing algorithm was applied to the videos of multi-hole injector and was found to be able to distinguish between videos that had fuel coverage events and those that did not. Manual inspection of the relevant videos was initially required to ensure that processed algorithm was performing satisfactory.

Results and Discussion

Atmospheric conditions

High-speed video were first acquired at atmospheric temperature and pressure. Figure 3 shows the injection process under these initial conditions. The focus of this research is the end of injection (EOI) so the sequence begins here. Typical injections begin to destabilise with disruptions in the spray pattern towards the trailing end. The sequence below (top row) shows what appears to be the end of an injection event that leaves only a few slow moving deformed droplets hanging in the air before falling away from the nozzle. It is known that slow moving and deformed droplets are not able to mix fully with the air inside the engine which can lead to poor combustion and increased emissions. The main problem with this particular injection even becomes apparent in the second row of images. Here, fluid is observed emerging from the orifice through either expansion from thermal inertia, or maybe residual fluid momentum from injection or pressure gradients about the injector tip. Gas is clearly seen expanding out of the orifice along with the fuel, before the liquid settles and spreads across the surface so leave a pool of fuel approximately 470 µm in diameter. The estimated area of coverage is indicated by the white ellipse. Given the fact that this surface is at an angle, and by assuming the fuel coverage is circular, the larger diameter was estimated to be the diameter of the fuel coverage which gives a fuel coverage area of 0.69 mm^2.

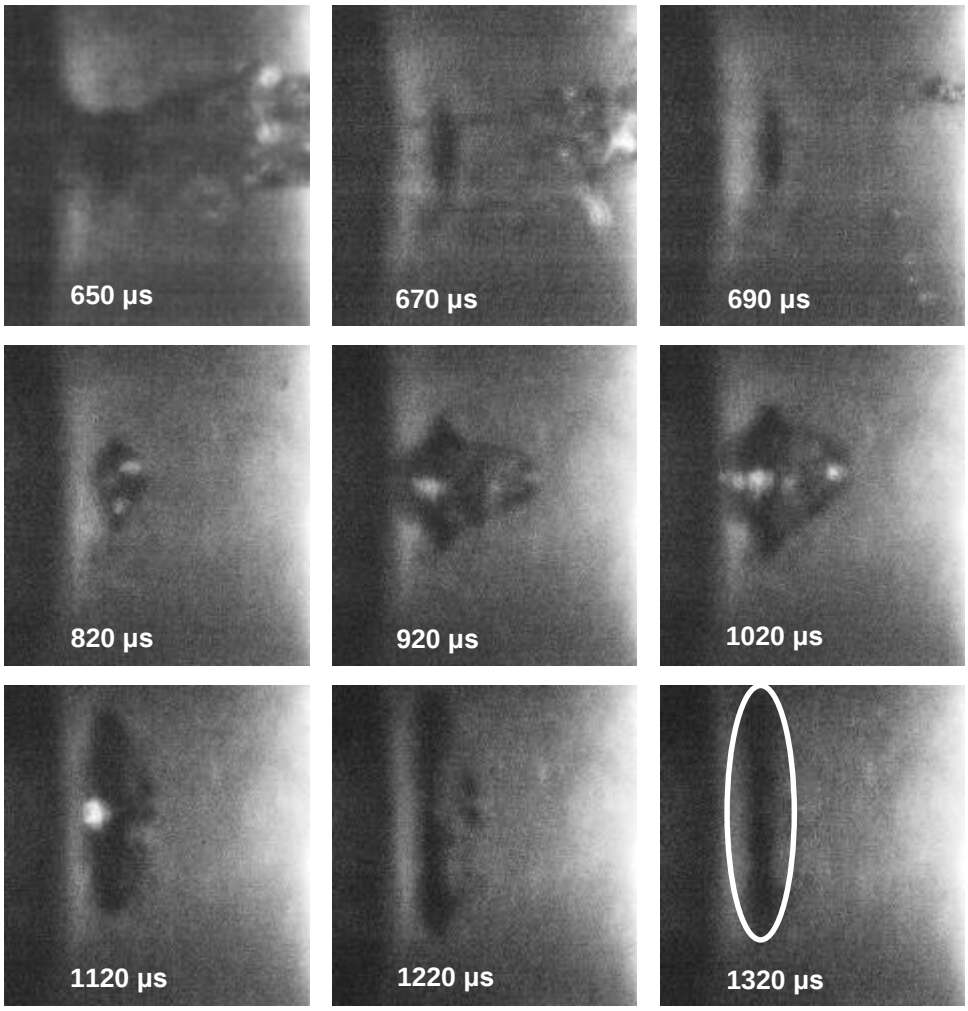

Figure 2: Injection at atmospheric pressure and 400 bar rail pressure. The first row shows the end of injection where droplets or spray are no longer visible (150-190 µs ASOI). The second row (320-520 µs ASOI) shows some post-injection fuel discharge that emerges with a bubble that then begins to spread across the surface. The third row (620-820 µs ASOI) shows this fuel has now spread out and covered the orifice. Estimated diameter is approx. 470 µm. This fuel is likely to remain until the emergence of the next fuel spray which is likely to hinder atomisation. Estimated fuel coverage area of 0.69 mm^2

High pressure conditions

Figure 3 shows an image sequence from the end of injection at elevated in-cylinder pressure. Images acquired at elevated pressures show more distortion in the form of blurring due to refractive index gradients of the gaseous

medium that the light is being integrated over. As a result, a compromise on clarity is always required in order to investigate the fluid dynamics at conditions that are representative of normal engine operation. This set of images was acquired at 40 bar ICP and 400 bar injection pressure. The first row of images shows the fully developed spray at 560 µs ASOI then towards the end of the spray (620-660 µs), we observed an increase in dispersion angle, an apparent reduction in flow rate and a splashing and swirling effect towards the end of the injection. No fuel was deposited onto the injector surface at this stage. The second row of images shows the appearance of a slowly growing white area around the dark orifice that is found to be surface bound fuel scattering the laser light. This appearance is typical for our method and consistently showed the presence of liquid on the metal surface. This post-injection fuel emerges slower and the presence of gas is less obvious when compared to observations at atmospheric conditions. The final row of images shows the white ring of scattered light growing in size at a higher rate than the previous row of images. The edge of the white ring is taken to be the edge of the fluid which shows a good contrast with the light reflected from the injector surface that is detected around the fluid perimeter. We observed fuel spreading across the surface to give a coverage diameter of approximately 310µm. The key differences in fluid behaviour here are that the area of the post-injection fuel coverage is greatly reduced, and so the volume of fuel remaining around the orifice is as well. By the previous method we arrived at an estimated coverage area of 0.31mm^2

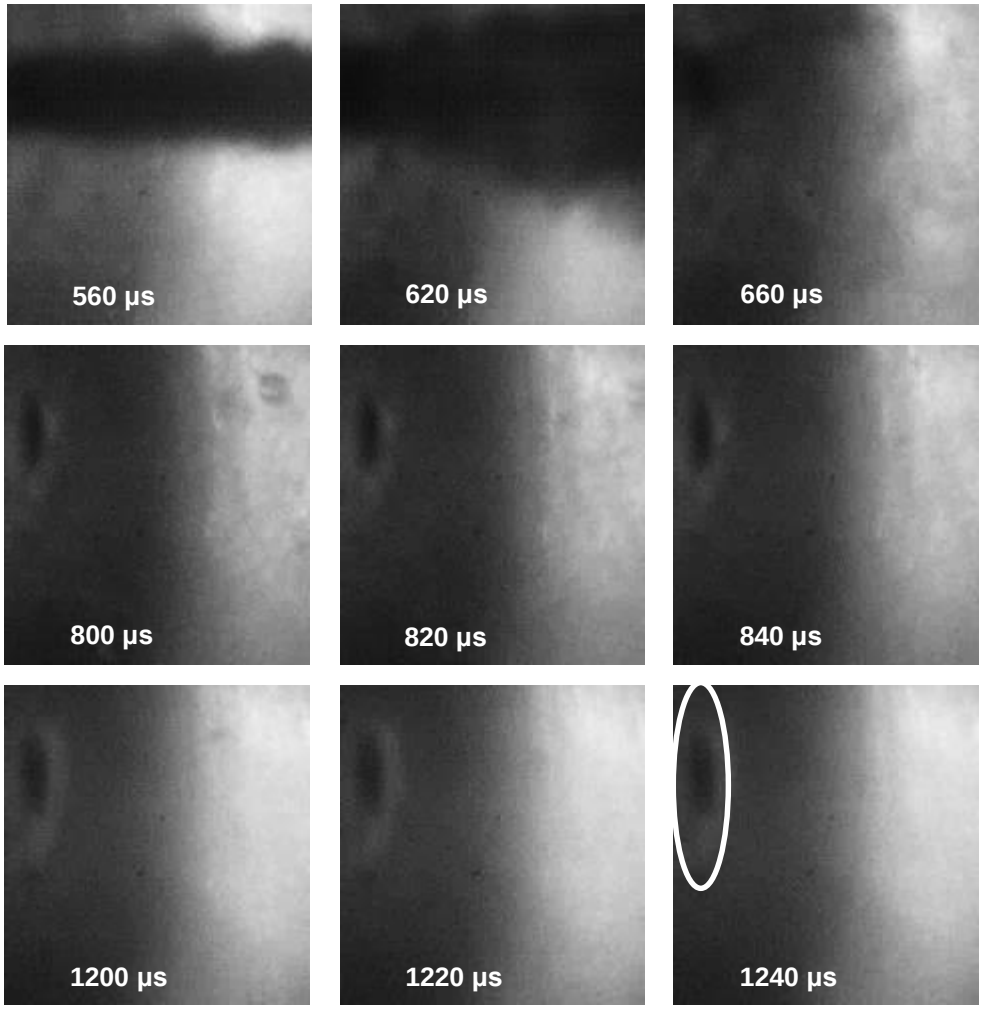

Figure 3: Image sequence showing the end of injection for a fuel spray at 400 bar injection pressure and 40 bar in-cylinder pressure. The first row of images shows the fully developed spray at 560 µs ASOI. We observed an increase in dispersion angle, an apparent reduction in flow rate and a splashing effect towards the end of the injection. The second row of images shows the appearance of a slowly growing white area around the dark orifice that is found to be surface bound fuel scattering the laser light. The white ring is light scattered by the surface bound fuel which we observed spreading across the surface of the injector. This appearance is typical for our method and consistently showed the presence of liquid on the metal surface. The final row of images shows the white ring of scattered light growing in size at a higher rate than the previous row of images. We observed fuel spreading across the surface to give a coverage diameter of approximately 310µm. The key differences in fluid behaviour here are that the area of the post-injection fuel coverage is greatly reduced, and so the volume of fuel remaining

around the orifice is as well. A reduction of the extent of fuel coverage is seen when the in-cylinder pressure is increased. Final coverage area was estimated at 0.31mm^2.

Increasing injection pressure

Figure 4 shows a similar image sequence from the end of injection at ICP of 40 bar and an elevated injection pressure of 1000 bar. The same end of injection behaviour is seen as in Figure 3 with the dispersion angle increasing and the deterioration of the spray into vapour at 560 µs ASOI. The splashing of fuel blocks the field of view and hinders subsequent observations due to light refraction by the vapour. Just 20 µs later, post injection fuel emerges from the orifice again, much faster than at lower injection pressures. This is most likely due to the increased fluid momentum which is a function of injection pressure. This fuel surges out of the orifice and splashes onto the injector surface (620 µs ASOI) and then another post injection event begins at 700 µs ASOI. The final row of images from 740-1000 µs ASOI shows the last residual fuel expand out of the orifice and spread over the nearby metal surfaces as was previously observed for lower injection pressures. The white area in the final 2 images is notably larger than the coverage at 400 bar for the same ICP and is comparable to the area in Figure 2 at around 460 µm.

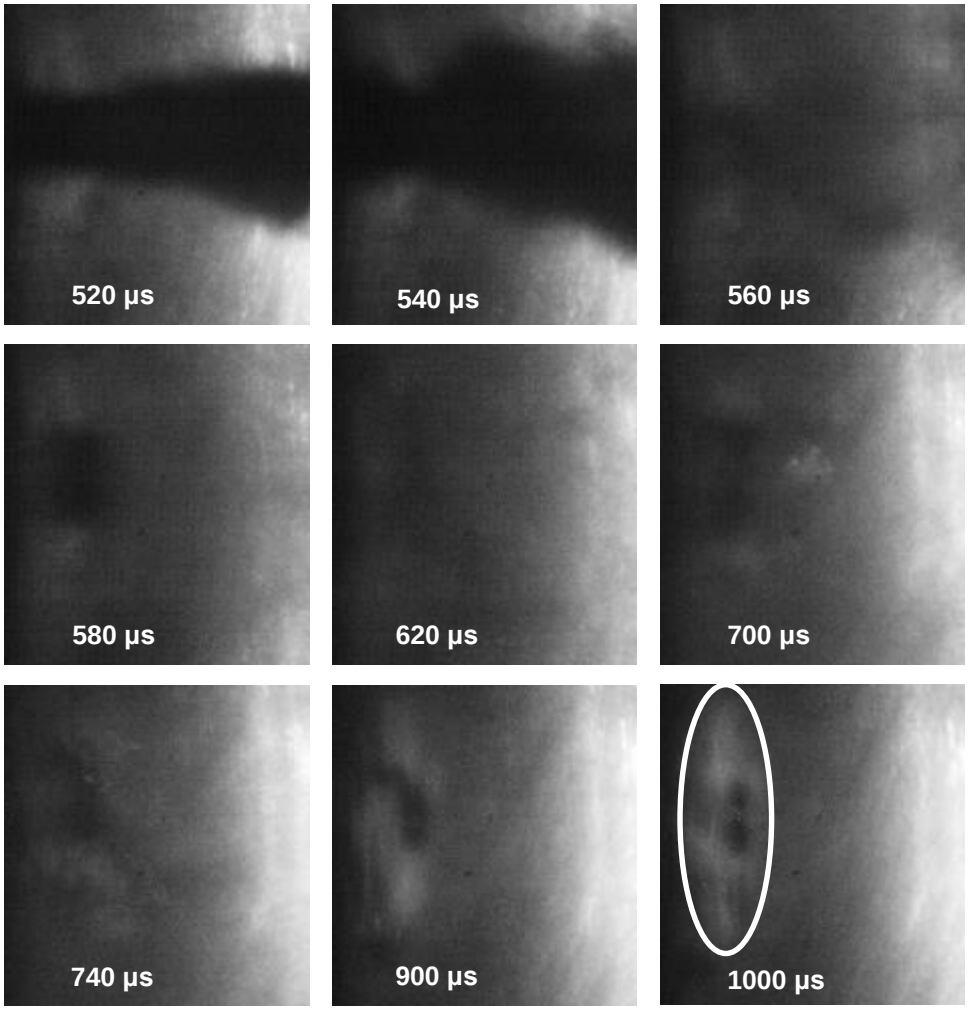

Figure 4: Image sequence showing the end of injection for a fuel spray at 1000 bar and 40 bar in-cylinder pressure. The increased injection pressure results in a much larger volume of post-injection fuel than 400 bar injection pressure, resulting in a much greater area of coverage comparable to the sequence recorded under atmospheric conditions in Figure 2. The second row of images from 580-700 µs ASOI shows very poor visibility due to the obstruction of the field of view my the fuel splashing and misting seen at the image labelled 560 µs. The area of final coverage is estimated by the white ellipse. Given the fact that this surface is at an angle, and by assuming the fuel coverage is circular, the longest diameter can be used to estimate the diameter of the fuel coverage which gives a coverage area of 0.66mm^2

Increasing In-cylinder pressure

Figure 5 shows an image sequence recorded at 80 bar ICP and 1000 bar injection pressure. Refractive index gradients are very steep and result in images that are harder to interpret. This example has improved clarity so

will be used to demonstrate some various modes of fuel coverage as well as the operating condition dependence. The first image at 570 µs ASOI shows the spray fully developed. The dispersion angle increases as in the previous image sequences but then almost all of the available light is obscured until 800 µs where we regained visibility to see the spray deteriorating and splashing onto the metal surface at 900 µs ASOI. A post-injection fuel surge begins at 940 µs ASOI and develops through to 1020 µs ASOI with further fuel splashing observed. At 1140 µs ASOI we observed another post injection fuel surge that appears to be running down the metal surface of the injector, likely due to gravity. What was interesting to note was that this fuel spreading along the metal surface is likely to interfere with the fluid dynamics at the adjacent orifice (indicated by the white arrow). Estimation of the final coverage area is less accurate for this example as there is a mass of fuel towards the lower part of the coverage area. The main surface bound fuel covered an area of approximate 0.36mm^2. Although it is not shown here, we also observed an increased incidence of fuel surges travelling vertically which we hypothesise is due to the greater influence flow motion can have at elevated pressures due to increased fluid momentum of the in-cylinder gas.

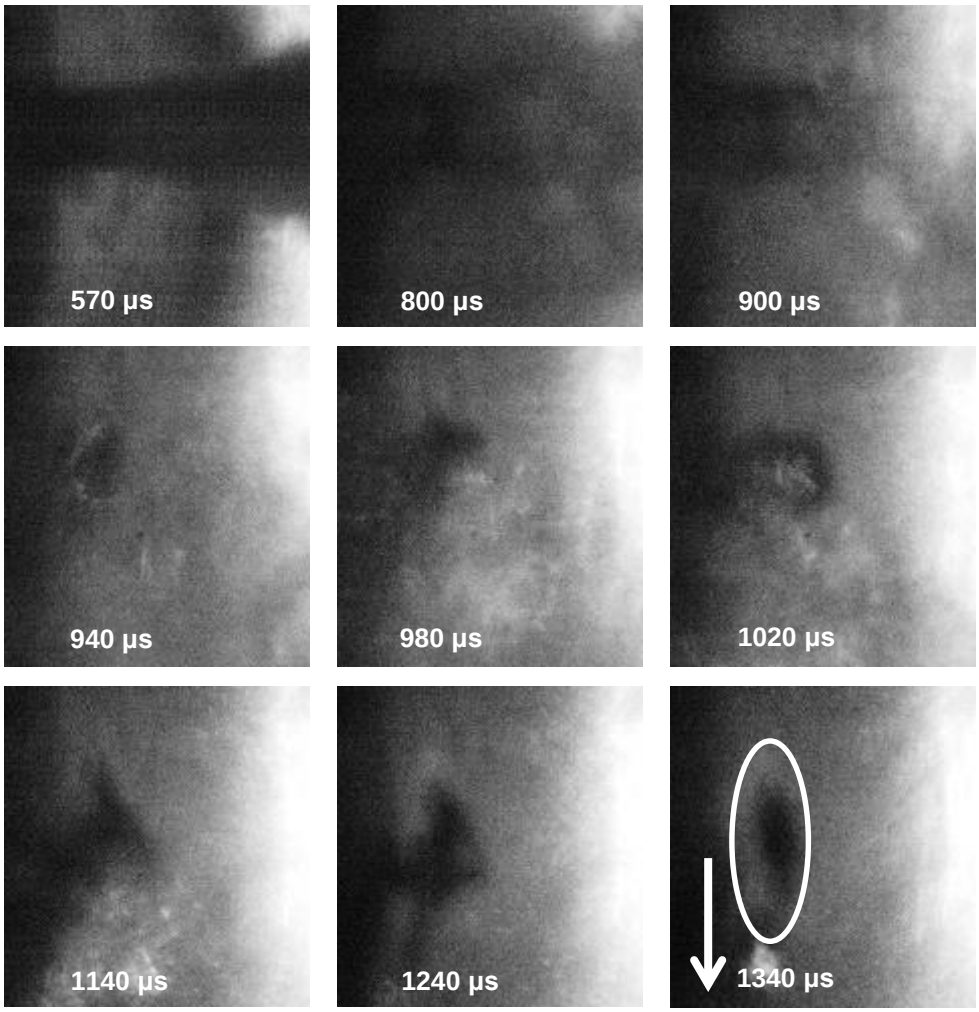

Figure 5: Image sequence from fuel spray at 1000 bar injection pressure and 80 bar ICP. Key observations include an apparent reduction in the rate of post injection, slow splashing and fuel surging is apparent. A very large volume of fuel comes out after the end of injection that appears to clear away faster than with lower pressures. An estimate in the final coverage area is at least 0.37 mm^2.

We observed several different modes of fuel coverage. One of which we propose is linked to the closing of the needle. Here, we noted cavitation effects which are likely due to the local velocity increase experienced by the fuel as the needle closes and the cross sectional area of the flow is reduced. This increase in fluid velocity will induce a perturbation in the flow that will manifest with a widening of spray angle and a reduction of spray velocity to the point where the liquid is stationary. The liquid will then fall onto the injector tip surface on and around the orifice. A swirling motion is often noted within the fuel which is residual from the fluid flow inside the common rail system.

Another mode was observed under higher injection pressures where we noted increased frequency of fuel discharge that is seen to occur long after the needle has closed. In this mode, post-injection fuel is left on the injector surface at a later stage than the previous mode so any fuel that emerges from the orifice can only be a result of the following hydrodynamic effects:

- Fuel expansion inside the sac volume due to thermal expansion
- Differential pressure through the observed orifice to the combustion chamber during the expansion stroke
- Differential pressure between neighbouring orifices due to air flow motion around the injector tip

A third mode is described relating to the spreading of fuel. This is delivery of fuel to the area around an orifice by one of two phenomena. The first is from lateral spreading caused by the vortex motion known to be formed by high velocity sprays, this spreading is observable by the area of higher intensity seen growing around the orifice. Other fuel spreading can be due to gravity, where fuel from a neighbouring orifice creeps along the surface and reaches the orifice being visualised. This mechanism can be linked to the fuel surge or splashing modes in that fuel creeping onto one orifice could have originated from a neighbouring orifice by one of the former modes. It should be noted that the three fluid dynamic modes are not discrete. Overlap was often noted, as well as multiple modes coinciding or even following on from each other. For example, large volume of post-injection fuel could be discharged as it expands out of the orifice, often accompanied by expanding gases in the form of a bubble. Once this fuel lands on and around the orifice it is free to be spread by either gravity or flow motion around the injector tip. Some video clips were recorded that show all of the orifices simultaneously for an entire engine revolution. This data will form part of the further analysis

All of the image sequences presented have been recorded for the time up to around 1500 µs ASOI. In our study, we also generated data that confirmed that there were fuel spillage events that occurred long after the end of this time frame, in fact, we observed fluid dynamics in the near-nozzle region for one entire revolution of the optical engine and observed spillage events occurring throughout the cycle, particularly around 270° and sometimes close to when the next injection event would be occurring. This shows that under the surface-bound fuel is often still in the near-nozzle region when the subsequent injection event takes place. This is likely to interfere with spray formation.

Figure 6 shows a schematic of a fuel spillage event. This type of fuel spillage is observed long after the injection trigger at which point the needle would be fully closed. This schematic is more specific to fuel spillage that is observed after the closing of the injector needle. ‘End of injection’ is defined as the time period that starts when no more fuel can be seen emerging in the form of a spray and there are no visible droplets or spray.

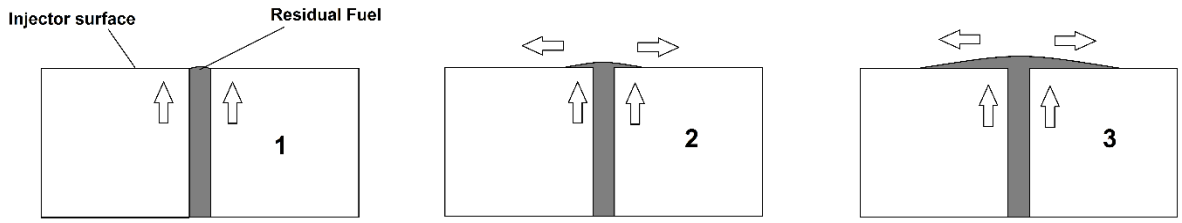

Figure 6: A schematic of a post-injection spillage event. 1: Residual fuel inside the orifice either still has momentum or is expanding out of the orifice. 2: Fuel contacts the injector tip surface and forms a curved liquid surface due to surface tension. 3: The liquid spreads across the surface due to capillary action where it can remain until a subsequent injection event.

Summary and Conclusions

The first optical investigation of fuel discharge and coverage at the microscopic level has been performed. Fuel spillage was classified into three modes relating to both the time of occurrence relative to injection, and the fluid dynamics that were observed. The extent of fuel coverage was related to operating conditions and found to be a function of injection pressure and a strong function of in-cylinder pressure. For a given in-cylinder pressure, varying the common rail pressure from 400-1000 bar allowed us to observe a reduction in the amount of fuel splashing onto the injector tip; an observation most likely due to the increase fluid momentum that causes greater liquid penetration and a resulting drop in fluid-surface interaction in and around the orifice. The amount of fuel that is delivered onto the injector surface after the end of injection increases as the injection pressure increases but the mode by which the fuel is deposited onto the surface is shifted towards being primarily by post injection fuel surges that occur when the injector needle is expected to be closed entirely.

We observed that the number of fuel coverage and spillage events increases with the ICP. This could be that the reduced pressure differential means there is less air resistance experienced by the fuel as it leaves the orifice meaning the fuel is more likely to experience liquid-surface interactions with the nozzle by way of friction resulting in increased coverage. An improved approach is to consider a control volume next to the injector tip. Here, increasing the gas pressure will result in an increased density of the gas which means the mass of a given volume is consequently higher which increases fluid momentum for a given direction of flow motion. This increased fluid momentum reduces liquid penetration and means that at higher ICP the fuel is more likely to interact with the surface around the nozzle. We found that, for a given injection pressure, the observed coverage events increased in frequency for all modes upon increasing the ICP. This control volume momentum hypothesis also affords an explanation for why lateral spreading of fuel was seen more at higher pressures, as well as the increased incidence of fuel surges travelling vertically on an expansion stroke. We observed that the flow motion has a greater influence on the fluid dynamics when the momentum associated with the flow is increased with the ICP. Finally, the post-injection fuel discharge we have studied will be exposed to high temperature zones during combustion so future work includes a look at fluid mechanics in the near nozzle region during combustion.

Acknowledgements

The authors would like to thank BP Formulated Products Technology and the EPSRC (EP/K020528/1) for financial support. The EPSRC Engineering Instrument Pool is also acknowledged for supplying equipment.

References

[1]. Delphi common rail system Brochures http://delphi.com/.
[2] Caprotti et al., SAE Paper No. 2005-01-3901
[3] Barker J et al., SAE Paper No. 2014-01-1387
[4] Reid J, et al., 2014, SAE Int J. Fuels Lubr. 7(2)
[5] Ferrari A, et al. 2013, Applied Energy, 103, pp. 243-255.
[6] Payri R, et al. 2011, Applied Energy, 88, pp.1130-1139.
[7] Olsen RE, et al., 1984, SAE Paer No. 841349,
[8] Sandquist H, et al., SAE Paer No. 2001-01-2028.
[9] Caprotti R, et al., 1993,. SAE Paper No. 932739.
[10] Lepperhoff G and Houben, M. 1993, SAE Paer No. 921032.
[11] Birgel A, et al., SAE Paper No. 2008-01-2383.
[12] Argueyrolles B, et al., SAE Paper No. 2007-01-1896